Journal of Cleaner Production 367 (2022) 132977

Contents lists available at ScienceDirect

Journal of Cleaner Production

journal homepage: www.elsevier.com/locate/jclepro

From biopolymer dissolution to CO_2 capture under atmospheric pressure - A molecular view on biopolymer@Ionic liquid materials

Mónica Lopes [a], André Cecílio [a], Marcileia Zanatta [a,b,**], Marta C. Corvo [a,*]

[a] i3N|Cenimat, Materials Science Department NOVA School of Science and Technology, NOVA University Lisbon, 2829-516, Caparica, Portugal
[b] Institute of Advanced Materials (INAM), Universitat Jaume I, 12071, Castellón, Spain

ARTICLE INFO

Handling Editor: M.T. Moreira

Keywords:
Chitosan
Chitin
NMR spectroscopy
Recyclability
Energy saving

ABSTRACT

Finding a cheap and easily recycling material that can capture CO_2 under atmospheric pressure (1 atm) is of paramount importance. In this context, combining ionic liquids (ILs) with abundant and natural materials, such as chitin-based biopolymers, appears as an interesting alternative. In this work, four acetate-based ILs were selected to explore the solubility of chitin, chitosan, and carboxymethyl-chitosan. Using carboxymethyl-chitosan and biopolymer monomer units as models, different Nuclear Magnetic Resonance (NMR) techniques, namely, ^{1}H, ^{13}C, nuclear Overhauser effect spectroscopy, and spin-lattice relaxation, were performed to evaluate the dissolution. Shrimp shells were used as a chitin source. Through a simple acid/base treatment, it was possible to remove minerals and proteins, and use it to prepare biopolymer@IL materials for CO_2 capture tests. Efficient CO_2 sorption capacity was observed upon bubbling CO_2 with a maximum of 2.32 $mmol_{CO2}/g_{sorbent}$. Under N_2 bubbling, the system demonstrated excellent recycling capacity using a room temperature procedure that outperformed aqueous amine solutions recycling. The absence of heating and vacuum recycling procedures, combined with the use of N_2 or compressed air is much more appealing for industrial applications.

1. Introduction

Chitosan (Cs) is the deacetylated form of chitin (Ct), that is the second most abundant biopolymer, just after cellulose. Ct is particularly common in exoskeletons of insects and crustaceans (Liu et al., 2018; Sun et al., 2019; Zhong et al., 2020). Both are linear heteropolysaccharides constituted by two monosaccharides, N-acetyl-D-glucosamine (*N*-(GlcNAc)) and D-glucosamine (GlcN) connected by β-1,4-glycosidic bonds (Mukhtar Ahmed et al., 2020). The main difference between them is the deacetylation degree, since Ct is mostly constituted by GlcNAc, while in Cs, GlcN is the predominant monosaccharide (>50%) (Pillai et al., 2009). Cs preserves the exceptional properties of Ct, such as biocompatibility, biodegradability, low toxicity, both are applied in fields of pharmaceutical, wastewater treatment, cosmetic, heavy metal chelation, heterogeneous catalyst, among others (Mukhtar Ahmed et al., 2020; Sun et al., 2019; Xie et al., 2006; Zhong et al., 2020). Despite their appealing advantages, many of these applications require the chemical modification of the biopolymers and/or the formation of stable homogeneous biopolymer solutions. However, due to the strong inter and intramolecular hydrogen bonding between the polymer chains, both native Ct and Cs are poorly dissolved in water, basic solutions, and common organic solvents. Ct can only be dissolved in specific solvents such as *N,N*-dimethylacetamide, hexafluoroacetone or hexafluoro-2-propanol, while acetic acid, formic acid, and some strong polar protic solvents, such as trichloroacetic acid exhibit good solvent abilities for Cs (Roy et al., 2017; Sun et al., 2019; Wang et al., 2010; Xie et al., 2006). However, these solvents are generally volatile, toxic, corrosive, and difficult to recover. In addition, the use of concentrated strong acids can reduce the molecular weight of biopolymer, by polymer chain fragmentation (Wang et al., 2010; Xu et al., 2016). Consequently, it is imperative to discover effective and sustainable solvents for Cs and Ct dissolution. This work aims at developing Cs and Ct derived materials for CO_2 capture, focusing on solutions of these polymers. With this goal, we conducted a detailed study on the molecular interactions that regulate both the solubilization and the behaviour towards CO_2, with the aim of providing both a rationalization and an optimization regarding the use of Cs/Ct solutions for CO_2 capture.

Ionic liquids (ILs) are ionic species with melting point under 100 °C,

* Corresponding author.
** Corresponding author. i3N|Cenimat, Materials Science Department NOVA School of Science and Technology, NOVA University Lisbon, 2829-516, Caparica, Portugal.
E-mail addresses: zanatta@uji.es (M. Zanatta), marta.corvo@fct.unl.pt (M.C. Corvo).

https://doi.org/10.1016/j.jclepro.2022.132977
Received 25 October 2021; Received in revised form 5 June 2022; Accepted 30 June 2022
Available online 4 July 2022

usually composed by organic cations and smaller inorganic or organic anions. Due to their unique properties, such as non-flammability, high thermal and chemical stability, ILs have attracted much attention as greener replacements for traditional solvents in different areas (Paiva et al., 2019; Trivedi et al., 2014; Yang et al., 2016). Their low vapor pressure is one of the most important feature resulting in less air pollution compared to volatile organic solvents (Mallakpour et al., 2012). Moreover, ILs have a remarkable ability to dissolve biopolymers, such as Ct and Cs (Feng et al., 2015; Ferreira et al., 2020; Li et al., 2012; Liu et al., 2018; Paiva et al., 2019; Shamshina, 2019). Xiao et al. considered that while the anions could interact with the hydrogen atoms of the hydroxyl and amine groups, the cations could interact with the oxygen and nitrogen of these same groups, respectively, destroying the hydrogen bonds in Cs and favoring the dissolution in ILs (Xiao et al., 2011).

Therefore, regarding the anions effect on Cs dissolution, some studies demonstrate that anions with ability to form hydrogen bond with –OH or $–NH_2$ of Cs are favourable to dissolution (Zhu et al., 2011). Thus, in general higher Cs dissolution capacity is observed for acetate-based ILs (up to 15 wt% in 1-ethyl-3-methylimidazolium acetate (EMI•OAc) compared chloride-based ILs (3 wt% in 1-butyl-3-methylimidazolium chloride (BMI•Cl)). In the same topic, Chen et al. determined the ILs' Kamlet-Taft β parameters to measure the hydrogen-bond-accepting ability, using ILs with different anions (Chen et al., 2011). Their results demonstrated an almost linear relation between the solubility of Cs and hydrogen-bond-accepting ability of the ILs. Regarding the cation effect, Sun *at al.* presented an important study by evaluating the effect of the cation alkyl chain size in imidazolium-based ILs (ImILs) with acetate anion (Sun et al., 2014a). Higher ability to dissolve Cs was observed in ImILs with shorter alkyl chain (2–4 carbons) compared to longer alkyl chain length (6–8 carbons), following the order: 1-butyl-3-methylimidazolium acetate (BMI•OAc) (15 wt%) > EMI•OAc (13.8 wt%) > 1-hexyl-3-methylimidazolium acetate (HMI•OAc) (12 wt%) > 1-octyl-3-methylimidazolium acetate (OMI•OAc) (7.4 wt%). Additionally, their results contributed to demonstrate that ImILs present higher ability to dissolve Cs than quaternary ammonium based ILs. So far, all these examples show that an adequate combination between cation and anion is requested to dissolve different amount of Cs.

Regarding Ct dissolution, despite similar studies have also been performed in literature, several disparities in the percentage of dissolution can be found, mainly due to provenance and type of Ct (β-chitin and α-chitin) (Prasad et al., 2009; Qin et al., 2010; Silva et al., 2011; Wang et al., 2010; Wu et al., 2008; Xie et al., 2006). Nevertheless, similar to what was observed in Cs dissolution, it is possible to state that ImILs are generally the most effective cations when compared to ammonium salts (Ferreira et al., 2020; Ma et al., 2020), being 16.66 wt% the maximum dissolution reported so far, obtained with EMI•OAc by Qin et al. (2010). Acetate ILs present higher dissolution capacity compared to other anions, since changing the anion results in lower dissolution: 3.3 wt% for EMI•Cl and only 1.5 wt% for EMI•Me_2PO_4 (Qin et al., 2010; Wang et al., 2010). Besides, mixtures of acetate-based ILs were tested by Gurau et al. however, no significant improvement in solubility can be described, resulting in 5.4 wt% Ct dissolution (Gurau et al., 2012).

The solvating ability of an IL depends on the interaction between the ILs' anion/cation and the biopolymer. Even with the increasing research in this area, just a few ILs have been reported as able to effectively dissolve polysaccharides, and rare experimental evidence of interaction sites between solvent and solute have been reported so far. In addition, a reliable and non-destructive technique able to evaluate the dissolution mechanism at the atomic level is still under investigation. The verification of biopolymers dissolution in ILs can be difficult. Generally, in translucid ILs, the dissolution of small amounts of Cs can be verified visually (Trivedi et al., 2014). However, the study of maximum dissolution or the use of dark ILs requires a different approach. Polarized optical microscopy (POM) (Li et al., 2012; Liu et al., 2013), X-Ray Diffraction (XRD) (Sun et al., 2014b; Tran et al., 2013), Wide-Angle X-ray Diffraction (WAXD) (Sun et al., 2014b; Xie et al., 2006), and Fourier-Transform Infrared Spectroscopy (FT-IR) (Ma et al., 2013; Sun et al., 2014b; Tran et al., 2013) are among the most used. Nuclear Magnetic Resonance can also be used to verify the dissolution and study the dissolution mechanism. In the last years, this technique has been applied to verify and monitor the dissolution of cellulose in ILs. So far only ^{13}C-{^1H} NMR techniques were used to evaluate the Cs dissolution in ILs, but no molecular interaction studies have been performed (Chen et al., 2011; Sun et al., 2014a).

Despite the several studies using ILs for CO_2 capture, only a few involving biopolymers dissolved in ILs were reported (Chen et al., 2014; Eftaiha et al., 2016b, 2017; Qaroush et al., 2017; Sun et al., 2014b; Xie et al., 2006). Xie et al. prepared a 10 wt% Cs/BMI•Cl solution to investigate the adsorption of CO_2 with Cs as reversible sorbent (Xie et al., 2006). Later, Chen et al. studied the CO_2 capture through mixtures between biopolymers and ILs, as well (Chen et al., 2014). The group prepared 4 wt% solutions of Cs/EMI•OAc and Ct/EMI•OAc and concluded that both systems could absorb a trace amount of CO_2 from the air physically and chemically. Recently, Eftaiha et al. studied the use of a Ct-acetate/DMSO binary system in CO_2 capture and discovered that, in the presence of DMSO, the Ct's C6 hydroxyl group reacts with CO_2 to form organic carbonate (Eftaiha et al., 2016a, 2016b, 2017; Qaroush et al., 2017). Despite the growing interest in the use of biopolymers for CO_2 capture, the regeneration of the materials is still an energy consuming process and, due to poor solubility, rare examples of Ct-based materials can be found (Eftaiha et al., 2016b). The energy penalty during the regeneration of the CO_2 capture materials is still a deal breaker for most CO_2 capture approaches (Osman et al., 2020). The contribution of total regeneration energy for using amine-based materials in direct air capture approaches has been determined to be around 60–70% of the cost (Elfving et al., 2021). In this context, to develop a competitive material, an ideal sorbent should be recycled with minimum energy consumption, preferably at room temperature.

Herein, we speculate the possibility of creating a cost-efficient and easy recyclable biopolymer@IL-based material. Our hypothesis is that by manipulating the composition of biopolymer/IL mixtures it is possible to achieve a material able to perform CO_2 uptake and release in an efficient manner. The main idea is to develop a CO_2 sorbent able to work under atmospheric pressure (1 atm) and room temperature, both for sorption and desorption process. In this work, four acetate-based ILs (BMI•OAc, EMI•OAc, choline acetate (Cho•OAc), 1,8-diazabicyclo [5.4.0]-undec-7-ene acetate (DBUH•OAc) – Fig. 1) were selected to prepare biopolymer@IL materials for CO_2 capture. Firstly, to properly select the materials, we investigated the solubility of Cs-based polysaccharides (Ct, Cs and Carboxymethyl-chitosan (CM-Cs)) in acetate-based ILs. The Cs-based polysaccharides used in this study range from natural sources, such as shrimp shells, to commercial compounds with a higher degree of treatment, such as CM-Cs. Using CM-Cs and polysaccharides monomers as models, the interaction between the biopolymer and the BMI•OAc was investigated through ^1H-NMR, ^{13}C-{^1H} NMR, nuclear Overhauser effect spectroscopy (NOESY) and spin-lattice relaxation (^1H T_1) experiments. All materials were tested in CO_2 capture and an efficient CO_2 sorption system was demonstrated with good recyclability and a low energy consuming process. Using an NMR approach, we rationalized the Ct and Cs dissolution mechanism in ILs and consequently provided evidence to understand the subsequent CO_2 sorption mechanism. This study allows an unprecedent and systematic molecular view from the design of the materials to the application in CO_2 capture.

2. Experimental section

2.1. ILs synthesis

General procedure: The following ILs BMI•OAc, EMI•OAc, Cho•OAc

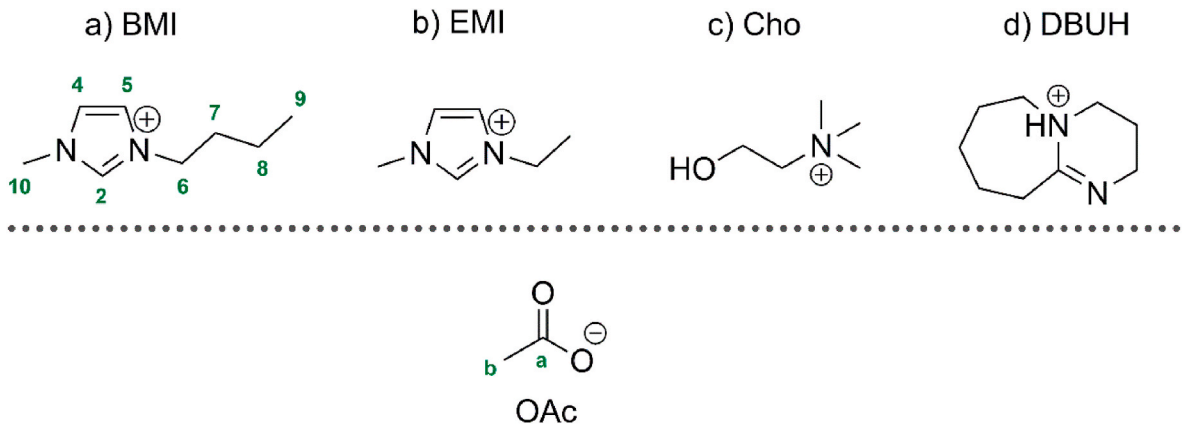

Fig. 1. ILs structures focused on this paper.

and BMI•Pro were obtained by simple anion exchange reaction of the corresponding chloride salt, according to the previous well-established procedure with small modifications (Zanatta et al., 2016). An ethanolic solution of the chloride salt (10 mmol, 20 mL) was slowly eluted through a column containing 6.00 g of Amberlyst A26 (OH-form), previously prepared with sodium hydroxide 1 mol L^{-1} (250 mL). To the eluted solution, 1 Eq of correspondent HX (acetic acid or proline) was added. The solution was stirred for 30 min, and the solvent was removed under reduced pressure. The final ILs were dried for 16 h, at 333 K, under vacuum. All the ILs were obtained with yield higher than 90% and at least 95% of purity.

The DBUH•OAc was prepared according to a previously reported procedure, with small modifications (Parviainen et al., 2015). In a round bottom flask, DBU (4 mmol) was added and purged with N_2. The acetic acid (4 mmol, 1 Eq) was slowly added dropwise at room temperature. After the addition, the reaction mixture was stirred for 30 min at 373 K.

2.2. Chitin treatment

Chitin samples from shrimp shell and from an industrial source were purified according to a procedure described in literature using acid and basic aqueous solution treatment, resulting in chitin from shrimp shell treated (CtST) and commercial chitin treated (CtCT) (Trung et al., 2020). In a typical experiment, shrimp shells were demineralized by continuously stirring with 0.80 mol.L^{-1} HCl solution (1:3.5 w/v) at room temperature for 12 h. The samples were then washed with water several times and then deproteinized with 0.75 mol.L^{-1} NaOH (1:2.5 w/v) at room temperature for 24 h. Finally, the samples were washed with demineralized water until neutrality.

2.3. Dissolution of biopolymers in ILs

The dissolution experiments were performed in glass flasks with a magnetic stirrer. The temperature was controlled digitally with a dry bath block. Starting at 298 K, the biopolymer was gradually loaded (1–2 wt%) into the solvent (D_2O, DMSO, neat IL or D_2O:IL). Subsequent portions of the biopolymer were added once the solution became clear. The complete list of prepared samples and respective names can be seen at supporting information Table S1. The temperature was increased to a maximum of 378 K. The dissolutions were evaluated by POM.

2.4. Sorption/desorption experiments

The samples for CO_2 capture were prepared using a mixture of solvents DMSO-d_6: D_2O (0.5 mL) and 100 mg of material (biopolymer@IL or IL). All the sorption experiments were performed through sample pressurization by bubbling CO_2 in 5 mm NMR glass tubes with a septum at atmospheric pressure and ambient temperature for around 30 min (830 cm^3 CO_2). The recycle experiments were carried out by bubbling N_2 for 15 min at room temperature.

3. Results and discussion

3.1. Understanding the dissolution: interaction study between IL and chitosan polysaccharides

3.1.1. Different biopolymers dissolution

The well-known ability of acetate anion to interact with CO_2, to dissolve biopolymers and their good chemical stability was explored to prepare the materials for this work (Kostag et al., 2020; Simon et al., 2017; Yang et al., 2019). The dissolution of five different biopolymers, starting from Ct directly from shrimp shell, commercial Ct, and Cs was tested in four IL acetate-based ILs (DBUH•OAc, Cho•OAc, EMI•OAc, BMI•OAc) (Table 1). All materials obtained from the dissolution of the biopolymer in ILs (called biopolymer@IL) were further applied in CO_2 capture. For this reason, 3 wt% was set as the target percentage for biopolymer dissolution, resulting in materials whose viscosity is more adequate to CO_2 diffusion compared to gels generally produced using higher biopolymer percentage.

From Table 1, it is possible to observe that both Ct samples were insoluble in Cho•OAc (entry 2–3). Therefore, a simple acid and basic treatment was conducted in Ct samples, yielding the solubilization of both treated Cts (entry 4–5). All the samples were analysed by ^{13}C CP-MAS to evaluate the degree of acetylation (DA). As observed in Fig. 2, no changes in DA can be observed, indicating the treatment was effective to remove minerals and proteins, but did not modify the chitin structure. The relation between the integral of CH_3 signal and the average of glucopyranosic ring carbons integrals was used to determine DA (see complete equation on supporting information) (Kasaai, 2010). In addition, from TGA analysis, no significant change in degradation temperature was observed (supporting information Fig. S1). These results demonstrated that a simple treatment allows the preparation of an economic and green material directly from shrimp shell, capable of attaining higher dissolution capacity. From this result, the next biopolymer@IL materials were prepared using Cs and the treated Cts (CtCT, CtST) which presented good solubility after treatment (Table 1, 4–14).

A deeper knowledge about the biopolymer@IL behaviour towards CO_2 capture requires a two-step analysis - we need first to rationalize the biopolymer's dissolution to later understand the mechanism of CO_2 sorption.

3.1.2. CM-Cs dissolution

After the successful preparation of biopolymer@IL materials, we focused on the biopolymer dissolution using different NMR techniques.

Chemical modifications of chitosan are usually performed to improve processability. Carboxymethylation is the predominant

Table 1
Dissolution experiments for Ct and Cs biopolymers in pure ILs.

Entry	Biopolymer	IL	Temp.(K)	Time (h)	wt% of biopolymer	Solubility
1	Cs	Cho·OAc	363–378	24	3.0	Partially Soluble[(a)]
2	CtC	Cho·OAc	363–378	24	1.5	Insoluble
3	CtS	Cho·OAc	363–378	24	1.5	Insoluble
4	CtCT	Cho·OAc	363–378	24	3.0	Soluble
5	CtST	Cho·OAc	363–378	24	3.0	Soluble
6	Cs	BMI·OAc	298–378	24	3.0	Soluble
7	CtCT	BMI·OAc	298–378	24	3.0	Soluble
8	CtST	BMI·OAc	298–378	24	3.0	Soluble
9	Cs	EMI·OAc	298–378	24	3.0	Soluble
10	CtCT	EMI·OAc	298–378	24	3.0	Soluble
11	CtST	EMI·OAc	298–378	24	3.0	Soluble
12	Cs	DBUH·OAc	363–378	24	3.0	Soluble
13	CtCT	DBUH·OAc	363–378	24	3.0	Soluble
14	CtST	DBUH·OAc	363–378	24	3.0	Soluble

[(a)] Sonication for 15 min.

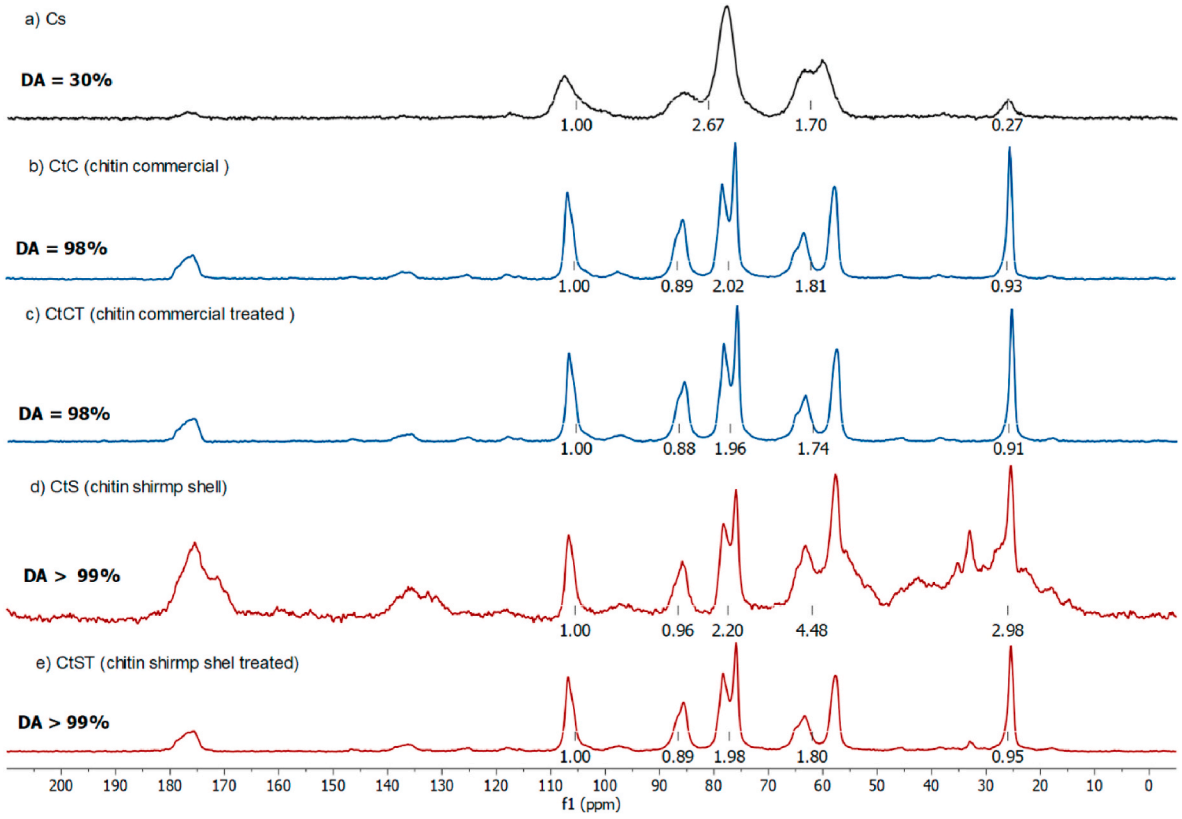

Fig. 2. ^{13}C CP-MAS NMR spectra (125 MHz, 298 K, 5 kHz) of biopolymers before and after treatment.

chemical modification that can enhance some properties such as solubility, biocompatibility, and biodegradability. Examples of carboxymethylation derivatives are *N,O*-carboxymethyl chitosan, *N*-carboxymethyl chitosan, and *O*-carboxymethyl chitosan (CM-Cs used in the current study) (Anitha et al., 2009). This amphoteric Cs derivative maintains all the main properties and applications of Cs, with the advantage of a larger dissolution window. While Cs only dissolves in acidic solvents, CM-Cs can be dissolved in water solutions (Kong et al., 2012), for this reason, CM-Cs was used as a study model. The maximal dissolution of CM-Cs in BMI•OAc was tested. CM-Cs is highly soluble in water; therefore, it was possible to dissolve 15 wt% CM-Cs in water, but not in bare (neat) BMI•OAc. Nevertheless, the CM-Cs dissolution became possible when the IL was previously dissolved in water (D_2O: BMI•OAc mixtures, (wt/wt): 150 mg IL/g D_2O), with a maximum solubility of 15 wt%. To evaluate the effect of CM-Cs concentration into the interaction with IL, the solutions CM-$Cs_{3wt\%}$@D_2O:BMI•OAc, CM-$Cs_{9wt\%}$@D_2O:BMI•OAc, and CM-$Cs_{15\ wt\%}$@D_2O:BMI•OAc were prepared. Different NMR techniques (Δδ, ^1H T_1, ^1H, and ^1H-NOESY) were employed to investigate the mechanism of dissolution.

In solution, slow movements of CM-Cs, as well as other biopolymers, enhance the spin-spin interactions, resulting in a faster relaxation of transverse magnetization (Foster et al., 2007). Consequently, it is very difficult to obtain the proton signals of CM-Cs. For this reason, as well as the low CM-Cs concentration, the ^1H-NMR spectrum of CM-$Cs_{3wt\%}$@D_2O:BMI•OAc, and ^1H HR-MAS NMR spectrum of CM-$Cs_{9wt\%}$@D_2O:BMI•OAc, don't show resolved signals of CM-Cs (see supporting information, Figs. S4 and S6, respectively). However, in the ^1H HR-MAS NMR spectrum of CM-$Cs_{15\ wt\%}$@D_2O is possible to detect signals related to the carboxymethyl protons of CM-Cs, between 2 and 5 ppm (see supporting information, Fig. S10).

Although the direct observation of CM-Cs' signals using NMR techniques is very difficult, the analysis of the changes in the solvent's chemical shift is possible. Thus, the chemical shift deviations in ^{1}H and ^{13}C-{^{1}H} NMR of D_2O:BMI•OAc and CM-$Cs_{3wt\%}$@D_2O:BMI•OAc, CM-$Cs_{9wt\%}$@D_2O:BMI•OAc, and CM-$Cs_{15\ wt\%}$@D_2O:BMI•OAc were calculated. Despite the absence of noticeable changes in ^{1}H NMR chemical shifts (see supporting information, Table S2) it's possible to observe that the ^{13}C-{^{1}H} NMR chemical shifts are more affected, presenting a more pronounced variation (Fig. 3 and Table S3).

For the three solutions, the chemical shift's behaviour was very similar, the cation's carbons suffer an upfield shift while the anion's carbons suffer a downfield shift. The upfield shift was higher in CM-$Cs_{15\ wt\%}$@D_2O:BMI•OAc solution, especially in C2 and C6 carbons where Δδ of −0.11 and −0.13 ppm, were respectively observed (Table S3). This result is in agreement with the previously reported by the groups of Chen and Sun (Chen et al., 2011; Sun et al., 2014a). According to the authors, the interactions between the –OH and/or –NH_2 groups of biopolymers with the imidazolium cation's protons lead to an increase of the electron density around the C2 to C10 atoms, and consequently to a decrease in the carbon chemical shift. Regarding the anion, a significant downfield was observed for Ca and Cb atoms, for all three solutions. With a variation between +0.30 and + 1.15 ppm for Ca atoms and +0.21 and + 0.87 ppm for the Cb atoms, suggesting that, in this solvent system, the anion plays a major role in the CM-Cs dissolution.

Similar results were obtained from ^{1}H T_1 relaxation time analysis (Fig. 4). The relaxation time T_1 is affected by the size of the molecule as well as the viscosity of the system. This measurement becomes an important tool, since the T_1 of small molecules significantly changes when they are interacting with a larger molecule. Fig. 4 shows the variation in ^{1}H T_1 relaxation times according to the increase of CM-Cs wt % in the D_2O:BMI•OAc solutions. The increase in the CM-Cs concentration leads to higher modifications in the T_1 values of imidazolium ring (H2, H4, and H5) and of anion (Hb) signals. The combination of ^{13}C chemical shift variation (Fig. 3) and the ^{1}H T_1 values (Fig. 4) indicate a modification in the chemical environment and molecular dynamics of imidazolium cation (polar region) and anion, suggesting a possible interaction with the biopolymer in these sites. The complete ^{1}H T_1 values can also be consulted in Table S2 (supporting information).

^{1}H, ^{1}H-NOESY analyses were performed to deeply study the interactions between the CM-Cs and the D_2O:BMI•OAc solvent system. HR-MAS ^{1}H, ^{1}H-NOESY contour map of CM-$Cs_{15\ wt\%}$@D_2O:BMI•OAc composite shows a weak correlation between water and the signals around 3.03–3.99 ppm. These signals are within the chemical shifts previously referenced as containing CM-Cs signals (Fig. S10), suggesting the polysaccharide interacts with water more strongly than with the IL.

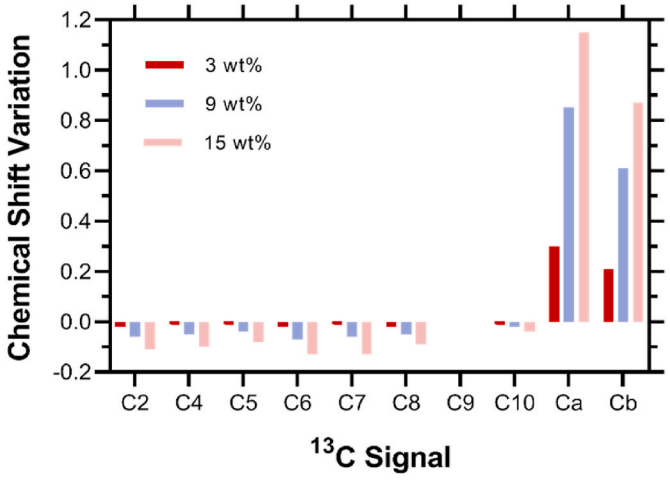

Fig. 3. ^{13}C NMR chemical shifts variation of CM-$Cs_{Xwt\%}$@D_2O:BMI•OAc solutions, where the ILs carbons (numbered according to Fig. 1).

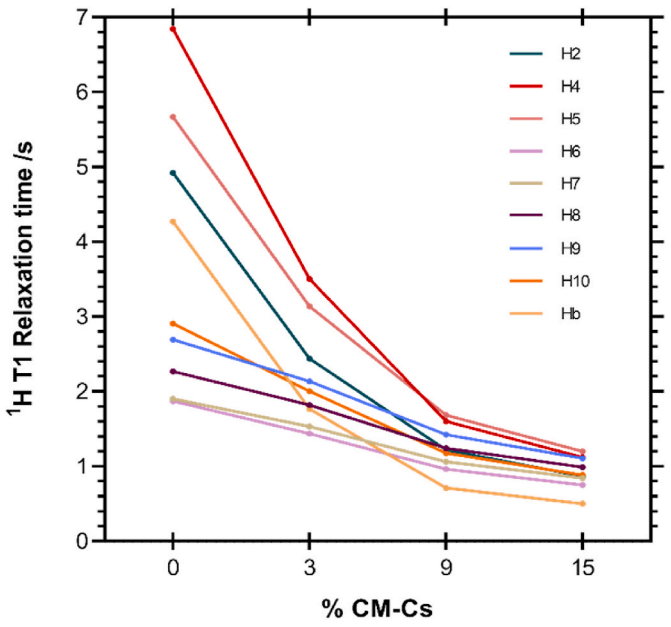

Fig. 4. Relation between CM-Cs concentration dissolution and the ^{1}H T_1 relaxation time of BMI•OAc, in the D_2O:BMI•OAc system, obtained from ^{13}C-{^{1}H} NMR (liquids) spectrum for $Cs_{3wt\%}$@D_2O:BMI•OAc composites, and from ^{13}C-{^{1}H} HR-MAS NMR spectra for $Cs_{9wt\%}$@D_2O:BMI•OAc and $Cs_{15\ wt\%}$@D_2O:BMI•OAc composites.

3.1.3. *Interaction between monomers and IL*

Ct and Cs are composed of different percentages of *N*-GlcNAc and GlcN monomers. For this reason, the interaction between BMI•OAc and each of these monomers was evaluated under NOESY analysis (Fig. 5 and S12). No interaction between IL and GlcN was observed (Fig. 5a). On the contrary, correlations between CH of *N*-GlcNAc and imidazolium ring of BMI•OAc (Fig. 5b), and correlations between the CH_3 of the (*N*-GlcNAc) and the N–CH_3 (H10) of cation (see Fig. S13) were detected. Indicating that the *N*-GlcNAc presents higher interaction with the IL than the GlcN, which can be more hydrophilic. In addition, the NOE pattern demonstrates a cross peak between DMSO-d_6, the IL cation (H10), and *N*-GlcNAc (CH), suggesting an interaction between all the components of the system (see Fig. S13). This is in accordance with our previous results, where interactions between IL and cellulose were observed by adjusting the concentration of solvent mixtures (IL/DMSO/H_2O) (Paiva et al., 2022). The interactions observed here allow us to understand the biopolymer dissolution and motivate our proposal of the CO_2 sorption mechanism in section 3.2.3.

3.2. *CO_2 capture evaluation*

3.2.1. *Effect of IL and polysaccharides variation*

The biopolymer$_{xwt\%}$@IL materials were dissolved in DMSO-d_6:D_2O and subjected to CO_2 bubbling (Table 2). The sorption capacity of all materials was evaluated by ^{13}C NMR technique, according to our previous reports (Corvo et al., 2013, 2015; Gonçalves et al., 2019; Simon et al., 2017, 2018; Zanatta et al., 2019, 2020b). The NMR spectroscopy allows quantifying the amount of CO_2 present through a direct relationship of the molar proportion between the IL and the absorbed CO_2. Generally, after the CO_2 sorption, two additional signals were observed: around 124 ppm, related to physisorbed CO_2 in the sample, and 159 ppm correspondent to a bicarbonate form (Fig. 6) (Gonçalves et al., 2019; Simon et al., 2017, 2018). Previous reports, using chitin acetate in DMSO-d_6 demonstrated the presence of signals at 124.7 and 157.4 ppm upon bubbling CO_2, which were ascribed to physically dissolved CO_2 in DMSO and the generated alkylcarbonate peak, respectively (Eftaiha et al., 2016a, 2016b). The same group has also demonstrated that adding

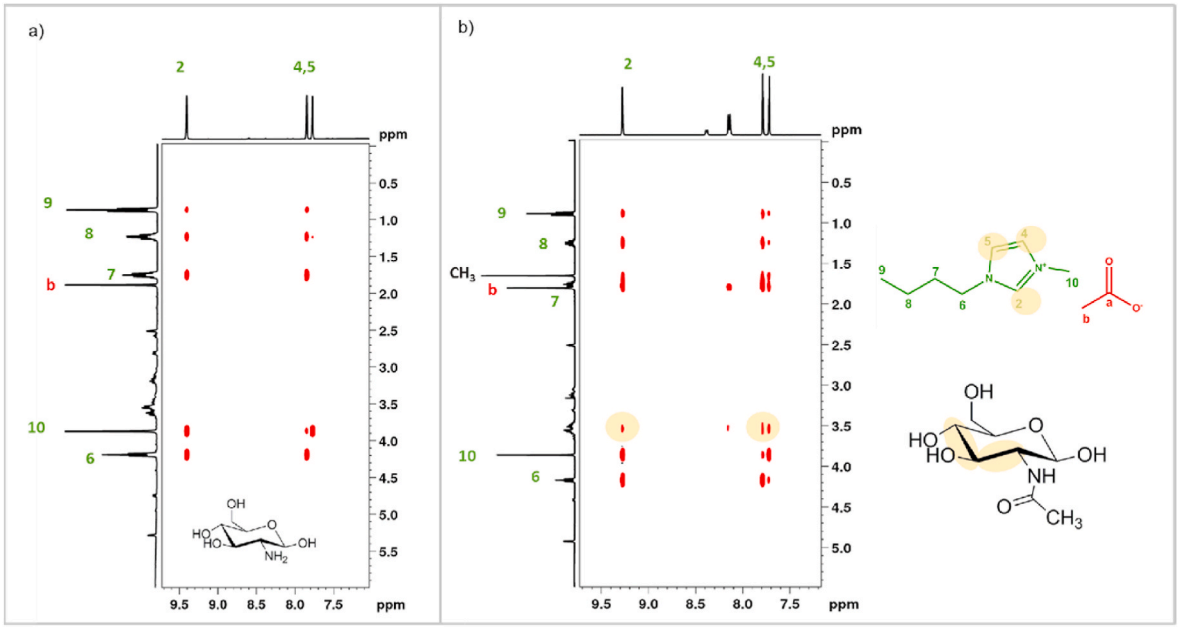

Fig. 5. $^{1}H,^{1}H$-NOESY contour map of BMI•OAc (0.5 mol L^{-1}, 800 ms of mixing time); mixture in DMSO-d_6 with: (a) GlcN (0.5 mol L^{-1}); *N*-GlcNAc (0.5 mol L^{-1}); Orange marks indicate the nuclei involved in the intermolecular interactions.

Table 2
CO_2 sorption capacity in biopolymer$_{xwt\%}$@IL materials.[a]

Entry	IL	Biopolymer (wt%)	mol_{HCO3-}/mol_{IL}	mol_{CO2}/mol_{IL}	$mol_{CO2\ total}/mol_{IL}$	$mmol_{CO2\ total}/g_{material}$
1	Cho·OAc	–	0.28	n.d[b]	0.28	1.66
2	Cho·OAc	CtST (3 wt%)	0.22	n.d[b]	0.22	1.31
3	Cho·OAc	CtCT (3 wt%)	0.28	0.08	0.36	2.14
4	Cho·OAc	CtCT (4 wt%)	0.30	0.09	0.39	2.32
5	Cho·OAc	CtCT (5 wt%)	0.30	0.04	0.34	2.02
6	Cho·OAc	Cs (3 wt%)	0.23	0.04	0.27	1.60
7	Cho·OAc	CtCT (3 wt%)[g]	0.31	n.d[b]	0.31	1.84
8	BMIm·OAc	–	0.34[c]	n.d[b]	0.34	1.71
9	BMIm·OAc	CtST (3 wt%)	0.35 [c]	n.d[b]	0.35	1.76
10	BMIm·OAc	CtCT (3 wt%)	0.30 [c]	n.d[b]	0.30	1.52
11	BMIm·OAc	Cs (3 wt%)	0.15	n.d[b]	0.15	0.73
12	EMIm·OAc	–	0.12 [c]	n.d[b]	0.12	0.74
13	EMIm·OAc	CtST (3 wt%)	0.10	0.08	0.18	1.03
14	EMIm·OAc	CtCT (3 wt%)	0.11	0.01	0.12	0.63
15	EMIm·OAc	Cs (3 wt%)	0.07	0.10	0.17	0.97
16	DBUH·OAc	–	0.14	0.20	0.34	1.55
17	DBUH·OAc	CtST (3 wt%)	n.d[b]	0.34	0.34	1.55
18	DBUH·OAc	CtCT (3 wt%)	n.d[b]	0.20	0.20	0.91
19	DBUH·OAc	Cs (3 wt%)	0.28	0.27	0.55	2.51
20	MDEA[d]	–	n.d[b]	0.10	0.10	0.81
21	MDEA[e]	–	0.82 (0.08)[f]	n.d[b]	0.90	7.33

[a] *Sorption conditions:* 0.2 g mL^{-1} solution of material in DMSO-d_6:D_2O (95:5 v/v) after 30 min of CO_2 bubbling at 298 K. HCO_3^- signal c.a. 158–159 ppm, CO_2 free c. a. 124 ppm.
[b] n.d. = not detectable.
[c] Signal at 155 ppm observed related to reaction between CO_2 and imidazolium cation (sorption <0.01 of CO_2–C2 zwitterionic complex).
[d] Solution of 30% (v/v) of MDEA in D_2O (0.150 mL of MDEA in 0.350 mL of D_2O).
[f] Signal in 160.3 and 157.7 ppm, relative to carbonate (CO_3^{2-}) e and bicarbonate (HCO_3^-) formation, respectively; (g) biopolymer + IL without previous dissolution.

water to chitin acetate/DMSO solution resulted in a peak at ca. 159 ppm (assigned to HCO_3^-) following CO_2 bubbling (Eftaiha et al., 2017). The sorption capacity was measured volumetrically within an *in situ* ATR-FTIR autoclave at 298 K, and 4.0 bar CO_2, resulting in capacity between 1.41 and 3.63 $mmol_{CO2}/g_{sorbent}$ (Eftaiha et al., 2016b). Herein, the use of acetate-based ILs may result in chitin acetate *in situ* following a similar sorption mechanism. The modification on chemical shift of the acetate (CH_3) in hydrogen and carbon spectra, before and after the CO_2 bubbling, should indicate a possible formation of chitin acetate (see supporting information Figs. S23 and S24). This result is also corroborated by the FTIR spectra, with the appearance of a characteristic band of bicarbonate around 1663 cm^{-1} when bubbling CO_2 (see supporting information Fig. S25).

Comparing 3 wt% with 4 wt% CtCT solutions, a small increase in sorption capacity is observed from 0.36 mol_{CO2}/mol_{IL} to 0.39 mol_{CO2}/mol_{IL} (Table 2, entries 3 and 4, respectively). However, the addition of more biopolymer to 5 wt% decreases the sorption capacity (0.34 mol_{CO2}/mol_{IL}), probably due to the increase in the viscosity of system. A similar result was previously reported, in which the increase from 3 wt% to 9 wt% in Ct/BMI•OAc system did not enhance the sorption efficiency (Sun et al., 2015). The effect of previous dissolution of CtCT in Cho·OAc was also evaluated, in comparison to the simple dispersion of

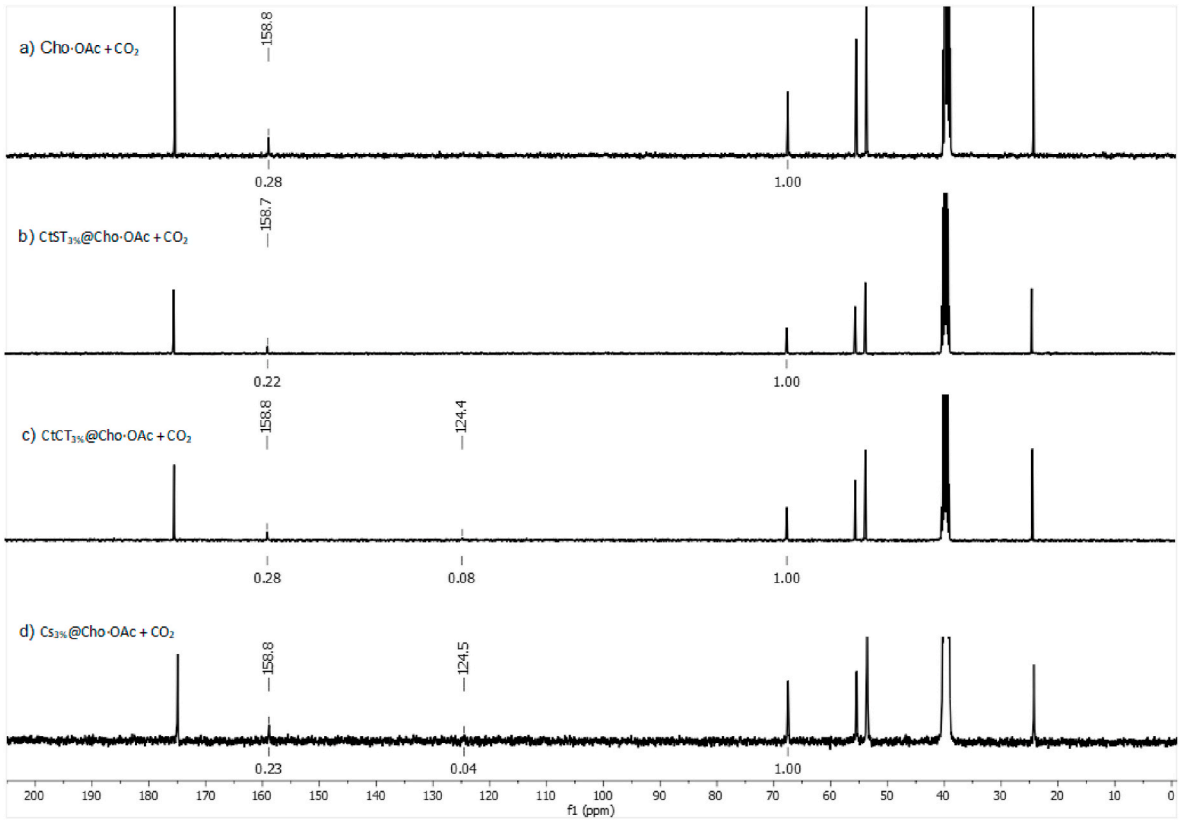

Fig. 6. ^{13}C-{^{1}H} NMR spectra (100 MHz, 298 K, inverse gated pulse sequence) of Cho·OAc based material 0.2 g mL^{-1} solution of material in DMSO-d_6:D_2O (95:5 v/v) after 30 min of bubbling CO_2: (a) pure IL; (b) $CtST_{3wt\%}$@Cho·OAc; (c) $CtCT_{3wt\%}$@Cho·OAc; (d) $Cs_{3wt\%}$@Cho·OAc.

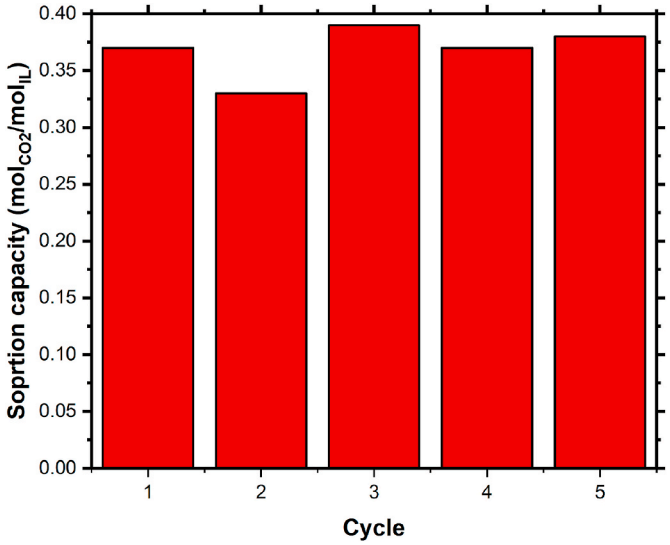

Fig. 7. Recycle test (sorption/desorption) for $CtCT_{3wt\%}$@Cho·OAc composite. Error of measurement <5%.

biopolymer. The sorption capacity of the material when the biopolymer was previously dissolved was 2.14 $mmol_{CO2\ total}/g_{material}$ compared to 1.84 $mmol_{CO2\ total}/g_{material}$ obtained for the mixture between IL and CtCT (Table 2, entries 3 and 7, respectively, and Fig. S16), proving the importance of previous solubilization to facilitate the interaction with CO_2.

BMI•OAc-based materials do not show any signal around 124 ppm, but exhibit a chemical shift around 159 ppm, indicating that all CO_2 dissolved in the samples is fully converted to bicarbonate species and consequently that the sorption kinetic is quicker in this IL compared to the others (Table 2, entries 8–12, Fig. S17). Furthermore, the presence of a small signal around 155 ppm, reveals CO_2 chemisorption by the C2 of the cation (Table 2, entries 8–10). The presence of acetate anion in ImIL allows the imidazolium ring reaction with CO_2 via carbene chemistry, this has previously been reported as the "acetate effect" in ImILs (Gurau et al., 2011).

No obvious trend between the type of biopolymer (CtST, CtCT, and Cs) and the amount of CO_2 captured was observed. However, for each IL there was always a biopolymer able to produce this increase. This could indicate that a combination of factors triggers the effectiveness of the sorption material, such as the interaction between cation, anion and biopolymers. However, according to the IL, the addition of 3 wt% of biopolymer was able to increase the sorption capacity compared to pure IL, which is the case for Ct in Cho•OAc, BMI•OAc and EMI•OAc, and Cs in EM•OAc and DBUH•OAc. This increase can be observed in the four ILs studied with different biopolymers, as is the case of the EMI•OAc that presents a sorption capacity of 0.11 mol_{CO2}/mol_{IL} for pure IL, and 0.18 mol_{CO2}/mol_{IL} for $CtST_{3wt\%}$@EMI•OAc and 0.17 mol_{CO2}/mol_{IL} $Cs_{3wt\%}$@EMI•OAc (Table 2, entries 12, 13, and 15 respectively, Fig. S18). Besides the increase in the sorption capacity, the use of the biopolymer in the sorption material can decrease the cost of IL-based absorbents.

Only physisorbed CO_2 was observed in $CtCT_{3wt\%}$@DBUH·OAc and $CtST_{3wt\%}$@DBUH·OAc materials (Table 2, entries 17–18). The $Cs_{3wt\%}$@DBUH·OAc composite demonstrated high sorption capacity, however, new signals appear compared to pure IL (Table 2, entries 16 and 19, respectively). These peaks may indicate degradation and/or by-products, probably because of the heating during the dissolution process (Fig. S19).

The $CtCT_{4wt\%}$@Cho·OAc presents the highest sorption capacity without any degradation, resulting in 2.32 $mmol_{CO2}/g_{sorbent}$, which is

remarkable for atmospheric pressure sorption. In our previous work we have demonstrated a maximum sorption capacity of 1.69 $mmol_{CO2}/g_{sorbent}$ for PIL@IL composites under 20 bar of CO_2 (Zanatta et al., 2020a). Despite the direct comparison with other works being difficult due to the specific experimental condition used in each study, the sorption capacity obtained here is comparable with significative literature examples. Composites formed between silica and BMI·OAc showed sorption capacity <2.39 $mmol_{CO2}/g_{sorbent}$ (298 K, 4 bar) (Anderson et al., 2015). The $CtCT_{4wt\%}$@Cho·OAc composite presents comparable sorption capacity to oligochitosan hydrochloride (CS·HCl) dissolved in DMSO (CS·HCl/DMSO), one of the most promising material previously described with a sorption ability of CO_2 2.41 $mmol_{CO2}/g_{sorbent}$ upon bubbling gas (Qaroush et al., 2017). In the present work, a similar sorption was obtained using a less manipulated starting material, *i.e.* using shrimp shell as Ct source.

With the purpose of comparing to an industrial methodology, CO_2 capture tests with MDEA were carried out (Mathonat et al., 1997). Using the same solvent of this work (DMSO-d_6:D_2O), the amine presents lower sorption capacity than the $biopolymer_{xwt\%}$@IL materials (Table 2, entry 20). However, analysing a 30% aqueous solution of MDEA, the CO_2 sorption capacity was 0.90 mol_{CO2}/mol_{MDEA} (Table 2, entry 21). In this case, no physisorption was observed and two signals at 157.5 ppm and at 160.5 ppm appeared after CO_2 bubbling. These were attributed to bicarbonate and carbonate, respectively. Despite the MDEA presenting the highest value found in all the experiments, the removal of CO_2 from amines is complicated and unsustainable at an environmental and economic level. Since the amine regeneration represents around 70% of the total cost of CO_2 capture, to prepare a solution easy to regenerate is still a challenge (Ochieng et al., 2012; Rochelle, 2009; Romeo et al., 2008). In this context, recycle tests were performed for selected samples.

3.2.2. Recycle tests

Cho•OAc samples demonstrate high sorption capacity and stability. For this reason, the $CtCT_{3wt\%}$@Cho·OAc was selected to evaluate the recyclability of the material. After each desorption cycle, ^{13}C NMR were performed to confirm the total desorption. Firstly, a recycle test heating the sample (323 K) under reduced pressure was performed (Xie et al., 2006), however, some CO_2 signal persisted in the NMR spectrum. In the same cycle, a second recycling methodology was tested, by bubbling N_2 into the solution at 298 K. In this case, the desorption was completely efficient (Fig. S20) (Zhu et al., 2017). After proceeding to a sequential CO_2 sorption cycle, a small decrease in sorption capacity was observed, probably due to the slight changes in solution concentration caused by the heating/vacuum procedure. Four more cycles were performed. From this point forward, the desorption was performed simply through N_2 bubbling and the sorption capacity was maintained constant (Fig. 7 and S23). Even more interesting, the same recycle procedure was performed for aqueous solution of MDEA 30% (v/v) and no efficient desorption was obtained. This result is extremely important since the absence of heating and vacuum recycling procedures represents a significant lowering in the overall cost, which is much more appealing for industrial applications (Fig. S22), making biopolymer@IL materials a potential candidate to compete with other commercially available compounds in the market. Moreover, the regeneration of these materials is also possible bubbling compressed air instead of pure N_2 (see supporting information), which is even a more cost-effective recycling option.

3.2.3. Mechanism proposal

Combining the previous rationalization of the biopolymer dissolution and the CO_2 capture results, a sorption/desorption mechanism was proposed (Fig. 8). Considering the interaction between cation/anion/biopolymer and the possibility of an equilibrium shift through N_2 addition, the formation of chitin acetate *in situ* with the sorption of CO_2 is suggested. In this case, the CO_2 interacts with the water naturally present in the ILs, yielding the HCO_3^- and protonating the NH of polysaccharide. The acetate ion is working as counterion of the biopolymer,

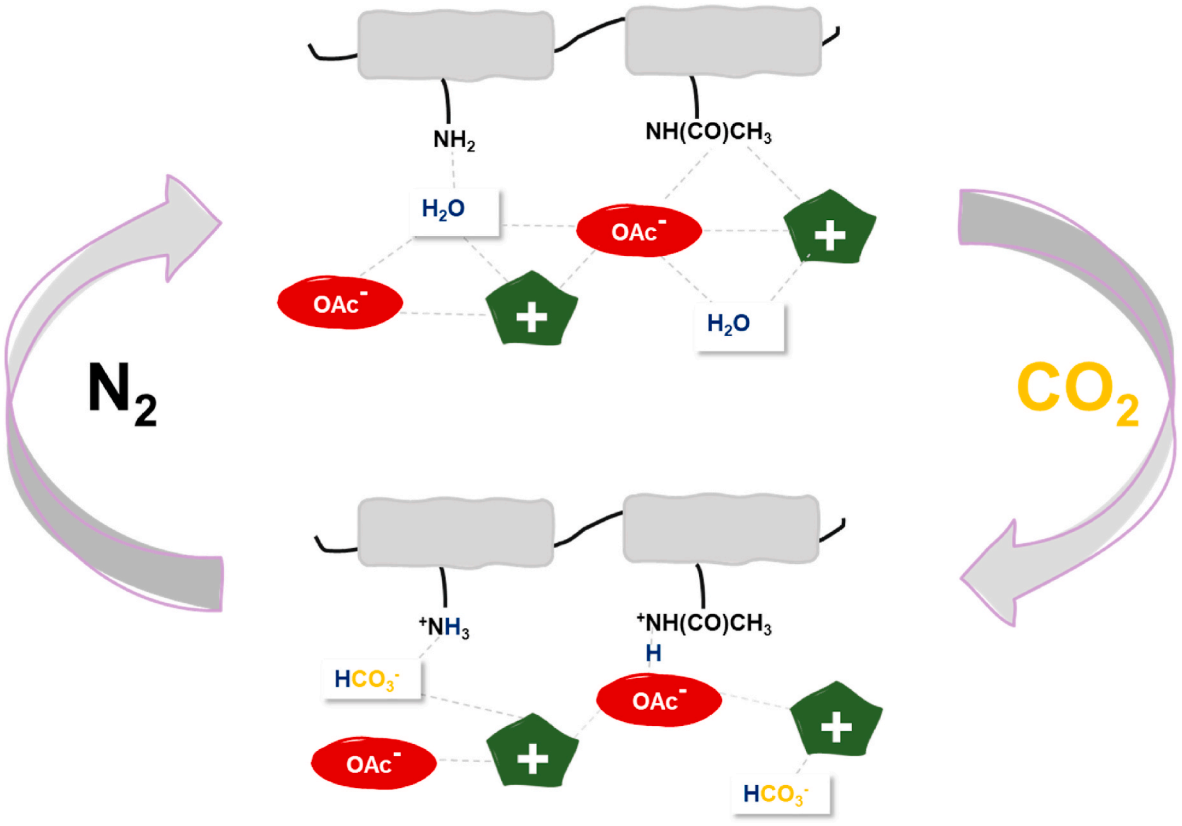

Fig. 8. Proposed mechanism for CO_2 sorption in biopolymer@IL composites.

balancing the net charge. Meanwhile, the HCO_3^- works as counterion of IL's cation. This behaviour is accentuated in chitin samples, due to higher percentage of GlcNAc monomer. The N_2 bubbling easily shifts back the equilibrium to regenerate the material and the biopolymers help the system to work as a buffer solution, since the basic pH of solution is almost unchanged before and after the CO_2. At the core of the mechanism of sorption-desorption is in fact an ion-swing process with OAC^- and HCO_3^- being exchanged between the IL and the biopolymer, mediated by the water interaction.

4. Conclusions

We report here the interactions between acetate-based ILs and chitosan family polysaccharides, studied from an NMR approach. The dissolution studies of CM-Cs in BMI•OAc demonstrated that the optimal amount of biopolymer in acetate-based ILs is 3 wt% since this amount keeps the viscosity of the system manageable for further studies and applications. Combining the results from dissolution studies of CM-Cs in BMI•OAc with the interaction evaluation between biopolymer monomers and BMI•OAc, is possible to state that although the anion plays a dominant role in the dissolution, the interaction strength between cation and anion is also an important feature to be considered. A methodology for capture of CO_2 at atmospheric pressure (1 atm) and room temperature was proposed combining the synergic effect of IL and biopolymer in the presence of DMSO. A maximum of 2.32 $mmol_{CO2}/g_{sorbent}$ of sorption capacity was observed upon bubbling CO_2. The system has demonstrated excellent recycling capacity with a simple methodology of N_2 bubbling at room temperature, which was also verified using compressed air, opening new possibilities to reduce the energy cost associated to the overall process. The need to reduce CO_2 emissions calls for urgent action, and as such the implementation of greener and economical approaches is highly desired. The main progress demonstrated here is the possibility use a cost-efficient material able work under atmospheric pressure and room temperature in the sorption and desorption process. Our data clearly emphasize the interest in pursuing a sustainable material for CO_2 capture, and consequently the importance of easily recyclable materials.

CRediT authorship contribution statement

Mónica Lopes: Investigation, Writing – original draft, Preparation, Writing – review & editing. **André Cecílio:** Investigation. **Marcileia Zanatta:** Conceptualization, Methodology, Validation, Writing – original draft, Preparation, Writing – review & editing, Visualization, Supervision. **Marta C. Corvo:** Conceptualization, Methodology, Validation, Resources, Writing – original draft, Preparation, Writing – review & editing, Visualization, Supervision, Funding acquisition.

Declaration of competing interest

The authors declare that they have no known competing financial interests or personal relationships that could have appeared to influence the work reported in this paper.

Acknowledgments

This work was funded by National Funds through FCT – Portuguese Foundation for Science and Technology, reference UIDB/50025/2020–2023 and PTDC/QUI-QFI/31508/2017, POR Lisboa and PTNMR (ROTEIRO/0031/2013; PINFRA/22161/2016), co-financed by ERDF through COMPETE 2020, Portugal, POCI and PORL and FCT through PIDDAC (POCI-01-0145-FEDER-007688). MZ acknowledges funding from European Union's Horizon 2020 research and innovation programme under the Marie Skłodowska-Curie grant agreement No 101026335. MCC gratefully acknowledges PTNMR&i3N for the former researcher contract and FCT for the current researcher contract (2021.03255.CEECIND).

Appendix A. Supplementary data

Supplementary data to this article can be found online at https://doi.org/10.1016/j.jclepro.2022.132977.

References

Anderson, K., Atkins, M.P., Estager, J., Kuah, Y., Ng, S., Oliferenko, A.A., Plechkova, N. V., Puga, A.V., Seddon, K.R., Wassell, D.F., 2015. Carbon dioxide uptake from natural gas by binary ionic liquid-water mixtures. Green Chem. 17, 4340–4354. https://doi.org/10.1039/c5gc00720h.

Anitha, A., Divya Rani, V.V., Krishna, R., Sreeja, V., Selvamurugan, N., Nair, S.V., Tamura, H., Jayakumar, R., 2009. Synthesis, characterization, cytotoxicity and antibacterial studies of chitosan, O-carboxymethyl and N,O-carboxymethyl chitosan nanoparticles. Carbohydr. Polym. 78, 672–677. https://doi.org/10.1016/j.carbpol.2009.05.028.

Chen, Q., Xu, A., Li, Z., Wang, J., Zhang, S., 2011. Influence of anionic structure on the dissolution of chitosan in 1-butyl-3-methylimidazolium-based ionic liquids. Green Chem. 13, 3446–3452. https://doi.org/10.1039/c1gc15703e.

Chen, Y., Sun, X., Yan, C., Cao, Y., Mu, T., 2014. The dynamic process of atmospheric water sorption in [EMIM][Ac] and mixtures of [EMIM][Ac] with biopolymers and CO2 capture in these systems. J. Phys. Chem. B 118, 11523–11536. https://doi.org/10.1021/jp5091075.

Corvo, M.C., Sardinha, J., Casimiro, T., Marin, G., Seferin, M., Einloft, S., Menezes, S.C., Dupont, J., Cabrita, E.J., 2015. A rational approach to CO $_2$ capture by imidazolium ionic liquids: tuning CO $_2$ solubility by cation alkyl branching. ChemSusChem 8, 1935–1946. https://doi.org/10.1002/cssc.201500104.

Corvo, M.C., Sardinha, J., Menezes, S.C., Einloft, S., Seferin, M., Dupont, J., Casimiro, T., Cabrita, E.J., 2013. Solvation of carbon dioxide in [C $_4$ mim][BF $_4$] and [C $_4$ mim][PF $_6$] ionic liquids revealed by high-pressure NMR spectroscopy. Angew. Chemie Int. Ed. 52, 13024–13027. https://doi.org/10.1002/anie.201305630.

Eftaiha, A.F., Alsoubani, F., Assaf, K.I., Nau, W.M., Troll, C., Qaroush, A.K., 2016a. Chitin-acetate/DMSO as a supramolecular green CO2-phile. RSC Adv. 6, 22090–22093. https://doi.org/10.1039/c6ra03022j.

Eftaiha, A.F., Alsoubani, F., Assaf, K.I., Troll, C., Rieger, B., Khaled, A.H., Qaroush, A.K., 2016b. An investigation of carbon dioxide capture by chitin acetate/DMSO binary system. Carbohydr. Polym. 152, 163–169. https://doi.org/10.1016/j.carbpol.2016.06.092.

Eftaiha, A.F., Qaroush, A.K., Assaf, K.I., Alsoubani, F., Markus Pehl, T., Troll, C., El-Barghouthi, M.I., 2017. Bis-tris propane in DMSO as a wet scrubbing agent: carbamic acid as a sequestered CO2 species. New J. Chem. 41, 11941–11947. https://doi.org/10.1039/C7NJ02130E.

Elfving, J., Kauppinen, J., Jegoroff, M., Ruuskanen, V., Järvinen, L., Sainio, T., 2021. Experimental comparison of regeneration methods for CO2 concentration from air using amine-based adsorbent. Chem. Eng. J. 404, 126337 https://doi.org/10.1016/J.CEJ.2020.126337.

Feng, J., Zang, H., Yan, Q., Li, M., Jiang, X., Cheng, B., 2015. Dissolution and utilization of chitosan in a 1-carboxymethyl-3-methylimidazolium hydrochloride ionic salt aqueous solution. J. Appl. Polym. Sci. 132, 1–7. https://doi.org/10.1002/app.41965.

Ferreira, I.C., Araújo, D., Voisin, P., Alves, V.D., Rosatella, A.A., Afonso, C.A.M., Freitas, F., Neves, L.A., 2020. Chitin-glucan complex – based biopolymeric structures using biocompatible ionic liquids. Carbohydr. Polym. 247, 116679 https://doi.org/10.1016/j.carbpol.2020.116679.

Foster, M.P., McElroy, C.A., Amero, C.D., 2007. Solution NMR of large molecules and assemblies. Biochemistry 46, 331–340. https://doi.org/10.1021/bi0621314.

Gonçalves, W.D.G., Zanatta, M., Simon, N.M., Rutzen, L.M., Walsh, D.A., Dupont, J., 2019. Efficient electrocatalytic CO2 reduction driven by ionic liquid buffer-like solutions. ChemSusChem 12, 4170–4175. https://doi.org/10.1002/cssc.201901076.

Gurau, G., Rodríguez, H., Kelley, S.P., Janiczek, P., Kalb, R.S., Rogers, R.D., 2011. Demonstration of chemisorption of carbon dioxide in 1,3-dialkylimidazolium acetate ionic liquids. Angew. Chem. Int. Ed. 50, 12024–12026. https://doi.org/10.1002/anie.201105198.

Gurau, G., Wang, H., Qiao, Y., Lu, X., Zhang, S., Rogers, R.D., 2012. Chlorine-free alternatives to the synthesis of ionic liquids for biomass processing. Pure Appl. Chem. 84, 745–754. https://doi.org/10.1351/PAC-CON-11-11-10.

Kasaai, M.R., 2010. Determination of the degree of N-acetylation for chitin and chitosan by various NMR spectroscopy techniques: a review. Carbohydr. Polym. 79, 801–810. https://doi.org/10.1016/J.CARBPOL.2009.10.051.

Kong, X.P., Wang, J., Wang, C.J., Wu, X., 2012. Basicity, water solubility and intrinsic viscosity of carboxymethyl chitosan as a biofunctional material. Adv. Mater. Res. 531, 507–510. https://doi.org/10.4028/www.scientific.net/AMR.531.507.

Kostag, M., Pires, P.A.R., El Seoud, O.A., 2020. Dependence of cellulose dissolution in quaternary ammonium acetates/DMSO on the molecular structure of the electrolyte: use of solvatochromism, micro-calorimetry, and molecular dynamics simulations. Cellulose 27, 3565–3580. https://doi.org/10.1007/s10570-020-03050-8.

Li, L., Yuan, B., Liu, S.W., Yu, S.T., Xie, C.X., Liu, F.S., Shan, L.J., 2012. Clean preparation process of chitosan oligomers in gly series ionic liquids homogeneous system. J. Polym. Environ. 20, 388–394. https://doi.org/10.1007/s10924-011-0388-z.

Liu, D., Chen, Q., Li, M., Lou, B., Yu, R., Li, Z., Zhang, Y., 2018. Influence of carboxyl anion on the dissolution of chitosan in cholinium-based ionic liquids. In: AIP Conference Proceedings, 050015. https://doi.org/10.1063/1.5041206.

Liu, L., Zhou, S., Wang, B., Xu, F., Sun, R., 2013. Homogeneous acetylation of chitosan in ionic liquids. J. Appl. Polym. Sci. 129, 28–35. https://doi.org/10.1002/app.38701.

Ma, B., Qin, A., Li, X., He, C., 2013. High tenacity regenerated chitosan fibers prepared by using the binary ionic liquid solvent (Gly·HCl)-[Bmim]Cl. Carbohydr. Polymer 97, 300–305. https://doi.org/10.1016/j.carbpol.2013.04.080.

Ma, Q., Gao, X., Bi, X., Han, Q., Tu, L., Yang, Y., Shen, Y., Wang, M., 2020. Dissolution and deacetylation of chitin in ionic liquid tetrabutylammonium hydroxide and its cascade reaction in enzyme treatment for chitin recycling. Carbohydr. Polym. 230, 115605 https://doi.org/10.1016/j.carbpol.2019.115605.

Mallakpour, S., Dinari, M., Mallakpour, Shadpour, Dinari, Mohammad, 2012. Ionic liquids as green solvents: progress and prospects. Green solvents II prop. Appl. Ion. Liq. 1–32. https://doi.org/10.1007/978-94-007-2891-2_1.

Mathonat, C., Majer, V., Mather, A.E., Grolier, J.P.E., 1997. Enthalpies of absorption and solubility of CO2 in aqueous solutions of methyldiethanolamine. Fluid Phase Equil. 140, 171–182. https://doi.org/10.1016/s0378-3812(97)00182-9.

Mukhtar Ahmed, K.B., Khan, M.M.A., Siddiqui, H., Jahan, A., 2020. Chitosan and its oligosaccharides, a promising option for sustainable crop production- a review. Carbohydr. Polym. 227, 115331 https://doi.org/10.1016/j.carbpol.2019.115331.

Ochieng, R., Berrouk, A.S., Peters, C.J., Slagle, J., 2012. Amine-based gas-sweetening processes prove economically more viable than the Benfield HiPure process. Oil Gas J. 1–26.

Osman, A.I., Hefny, M., Abdel Maksoud, M.I.A., Elgarahy, A.M., Rooney, D.W., 2020. Recent advances in carbon capture storage and utilisation technologies: a review. Environ. Chem. Lett. 192 19, 797–849. https://doi.org/10.1007/S10311-020-01133-3, 2020.

Paiva, T., Echeverria, C., Godinho, M.H., Almeida, P.L., Corvo, M.C., 2019. On the influence of imidazolium ionic liquids on cellulose derived polymers. Eur. Polym. J. 114, 353–360. https://doi.org/10.1016/j.eurpolymj.2019.02.032.

Paiva, T.G., Zanatta, M., Cabrita, E.J., Bernardes, C.E.S., Corvo, M.C., 2022. DMSO/IL solvent systems for cellulose dissolution: binary or ternary mixtures? J. Mol. Liq. 345, 117810 https://doi.org/10.1016/j.molliq.2021.117810.

Parviainen, A., Wahlström, R., Liimatainen, U., Liitiä, T., Rovio, S., Helminen, J.K.J., Hyväkkö, U., King, A.W.T., Suurnäkki, A., Kilpeläinen, I., 2015. Sustainability of cellulose dissolution and regeneration in 1,5-diazabicyclo[4.3.0]non-5-enium acetate: a batch simulation of the IONCELL-F process. RSC Adv. 5, 69728–69737. https://doi.org/10.1039/c5ra12386k.

Pillai, C.K.S., Paul, W., Sharma, C.P., 2009. Chitin and chitosan polymers: chemistry, solubility and fiber formation. Prog. Polym. Sci. 34, 641–678. https://doi.org/10.1016/j.progpolymsci.2009.04.001.

Prasad, K., Murakami, M. aki, Kaneko, Y., Takada, A., Nakamura, Y., Kadokawa, J. ichi, 2009. Weak gel of chitin with ionic liquid, 1-allyl-3-methylimidazolium bromide. Int. J. Biol. Macromol. 45, 221–225. https://doi.org/10.1016/j.ijbiomac.2009.05.004.

Qaroush, A.K., Assaf, K.I., Bardaweel, S.K., Al-Khateeb, A., Alsoubani, F., Al-Ramahi, E., Masri, M., Brück, T., Troll, C., Rieger, B., Eftaiha, A.F., 2017. Chemisorption of CO2 by chitosan oligosaccharide/DMSO: organic carbamato-carbonato bond formation. Green Chem. 19, 4305–4314. https://doi.org/10.1039/c7gc01830d.

Qin, Y., Lu, X., Sun, N., Rogers, R.D., 2010. Dissolution or extraction of crustacean shells using ionic liquids to obtain high molecular weight purified chitin and direct production of chitin films and fibers. Green Chem. 12, 968–997. https://doi.org/10.1039/c003583a.

Rochelle, G.T., 2009. Amine scrubbing for CO2 capture. Science 325, 1652–1654. https://doi.org/10.1126/science.1176731.

Romeo, L.M., Bolea, I., Escosa, J.M., 2008. Integration of power plant and amine scrubbing to reduce CO2 capture costs. Appl. Therm. Eng. 28, 1039–1046. https://doi.org/10.1016/j.applthermaleng.2007.06.036.

Roy, J.C., Salaün, F., Giraud, S., Ferri, A., Chen, G., Guan, J., 2017. Solubility of chitin: solvents, solution behaviors and their related mechanisms. In: Solubility of Polysaccharides. InTech. https://doi.org/10.5772/intechopen.71385.

Shamshina, J.L., 2019. Chitin in ionic liquids: historical insights into the polymer's dissolution and isolation. A review. Green Chem. 21, 3974–3993. https://doi.org/10.1039/C9GC01830A.

Silva, S.S., Duarte, A.R.C., Carvalho, A.P., Mano, J.F., Reis, R.L., 2011. Green processing of porous chitin structures for biomedical applications combining ionic liquids and supercritical fluid technology. Acta Biomater. 7, 1166–1172. https://doi.org/10.1016/j.actbio.2010.09.041.

Simon, N.M., Zanatta, M., Neumann, J., Girard, A.-L., Marin, G., Stassen, H., Dupont, J., 2018. Cation−Anion−CO 2 interactions in imidazolium-based ionic liquid sorbents. ChemPhysChem 19, 2879–2884. https://doi.org/10.1002/cphc.201800751.

Simon, N.M.N.M., Zanatta, M., dos Santos, F.P.F.P., Corvo, M.C.M.C., Cabrita, E.J.E.J., Dupont, J., 2017. Carbon dioxide capture by aqueous ionic liquid solutions. ChemSusChem 10, 4927–4933. https://doi.org/10.1002/cssc.201701044.

Sun, X., Huang, C., Xue, Z., Mu, T., 2015. An environmentally benign cycle to regenerate chitosan and capture carbon dioxide by ionic liquids. Energy Fuel. 29, 1923–1930. https://doi.org/10.1021/ef502585y.

Sun, X., Tian, Q., Xue, Z., Zhang, Y., Mu, T., 2014a. The dissolution behaviour of chitosan in acetate-based ionic liquids and their interactions: from experimental evidence to density functional theory analysis. RSC Adv. 4, 30282–30291. https://doi.org/10.1039/c4ra02594f.

Sun, X., Xue, Z., Mu, T., 2014b. Precipitation of chitosan from ionic liquid solution by the compressed CO2 anti-solvent method. Green Chem. 16, 2102–2106. https://doi.org/10.1039/c3gc42166j.

Sun, Y., Qing, M., Chen, L., Liu, J., Zhong, F., Jiang, P., Wang, G., Zhuang, L., 2019. Chitosan dissolution with sulfopropyl imidazolium Brönsted acidic ionic liquids. J. Mol. Liq. 293, 111533 https://doi.org/10.1016/j.molliq.2019.111533.

Tran, C.D., Duri, S., Harkins, A.L., 2013. Recyclable synthesis, characterization, and antimicrobial activity of chitosan-based polysaccharide composite materials. J. Biomed. Mater. Res. Part A 101 A 2248–2257. https://doi.org/10.1002/jbm.a.34520.

Trivedi, T.J., Rao, K.S., Kumar, A., 2014. Facile preparation of agarose-chitosan hybrid materials and nanocomposite ionogels using an ionic liquid via dissolution, regeneration and sol-gel transition. Green Chem. 16, 320–330. https://doi.org/10.1039/c3gc41317a.

Trung, T.S., Tram, L.H., Van Tan, N., Van Hoa, N., Minh, N.C., Loc, P.T., Stevens, W.F., 2020. Improved method for production of chitin and chitosan from shrimp shells. Carbohydr. Res. 489, 107913 https://doi.org/10.1016/j.carres.2020.107913.

Wang, W.T., Zhu, J., Wang, X.L., Huang, Y., Wang, Y.Z., 2010. Dissolution behavior of chitin in ionic liquids. J. Macromol. Sci., Part B: Phys. 49, 528–541. https://doi.org/10.1080/00222341003595634.

Wu, Y., Sasaki, T., Irie, S., Sakurai, K., 2008. A novel biomass-ionic liquid platform for the utilization of native chitin. Polymer (Guildf) 49, 2321–2327. https://doi.org/10.1016/j.polymer.2008.03.027.

Xiao, W., Chen, Q., Wu, Y., Wu, T., Dai, L., 2011. Dissolution and blending of chitosan using 1,3-dimethylimidazolium chloride and 1-H-3-methylimidazolium chloride binary ionic liquid solvent. Carbohydr. Polym. 83, 233–238. https://doi.org/10.1016/j.carbpol.2010.07.046.

Xie, H., Zhang, S., Li, S., 2006. Chitin and chitosan dissolved in ionic liquids as reversible sorbents of CO2. Green Chem. 8, 630–633. https://doi.org/10.1039/b517297g.

Xu, B., Li, Q., Zhuang, L., Wang, Q., Li, C., Wang, G., Xie, F., Halley, P.J., 2016. Dissolution and regeneration behavior of chitosan in 3-methyl-1-(ethylacetyl)imidazolium chloride. Fibers Polym. 17, 1741–1748. https://doi.org/10.1007/s12221-016-6747-6.

Yang, M., Zhao, W., Wang, S., Yu, C., Singh, S., Simmons, B., Cheng, G., 2019. Dimethyl sulfoxide assisted dissolution of cellulose in 1-ethyl-3-methylimidazoium acetate: small angle neutron scattering and rheological studies. Cellulose 26, 2243–2253. https://doi.org/10.1007/s10570-018-2218-0.

Yang, X., Qiao, C., Li, Y., Li, T., 2016. Dissolution and resourcfulization of biopolymers in ionic liquids. React. Funct. Polym. 100, 181–190. https://doi.org/10.1016/j.reactfunctpolym.2016.01.017.

Zanatta, M., Girard, A.L., Marin, G., Ebeling, G., Dos Santos, F.P., Valsecchi, C., Stassen, H., Livotto, P.R., Lewis, W., Dupont, J., 2016. Confined water in imidazolium based ionic liquids: a supramolecular guest@host complex case. Phys. Chem. Chem. Phys. 18, 18297–18304. https://doi.org/10.1039/c6cp03112a.

Zanatta, M., Lopes, M., Cabrita, E.J., Bernardes, C.E.S., Corvo, M.C., 2020a. Handling CO2sorption mechanism in PIL@IL composites. J. CO2 Util. 41, 101225 https://doi.org/10.1016/j.jcou.2020.101225.

Zanatta, M., Simon, N.M., dos Santos, F.P., Corvo, M.C., Cabrita, E.J., Dupont, J., 2019. Correspondence on "preorganization and cooperation for highly efficient and reversible capture of low-concentration CO $_2$ by ionic liquids. Angew. Chemie Int. Ed. 58, 382–385. https://doi.org/10.1002/anie.201712252.

Zanatta, M., Simon, N.M., Dupont, J., 2020b. The nature of carbon dioxide in bare ionic liquids. ChemSusChem 13, 3101–3109. https://doi.org/10.1002/cssc.202000574.

Zhong, Y., Cai, J., Zhang, L.-N., 2020. A review of chitin solvents and their dissolution mechanisms. Chin. J. Polym. Sci. 38, 1047–1060. https://doi.org/10.1007/s10118-020-2459-x.

Zhu, Q., Han, X., Cheng, C., Wu, C., 2011. Study on dissolubility of chitosan in four kinds of imidazole-based ionic liquids. Acta Polym. Sin. 11, 1173–1179. https://doi.org/10.3724/SP.J.1105.2011.10272.

Zhu, X., Song, M., Xu, Y., 2017. DBU-based protic ionic liquids for CO2 capture. ACS Sustain. Chem. Eng. 5, 8192–8198. https://doi.org/10.1021/acssuschemeng.7b01839.